Accepted Manuscript

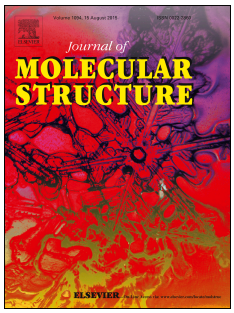

Gabapentin-base synthesis and theoretical studies of biologically active compounds: *N*-cyclohexyl-3-oxo-2-(3-oxo-2-azaspiro[4.5] decan-2-yl)-3-arylpropanamides and *N*-(*tert*-butyl)-2-(3-oxo-2-azaspiro[4.5]decan-2-yl)-2-arylacetamide derivatives

Mahboobe Amirani Poor, Ali Darehkordi, Mohammad Anary-Abbasinejad, Marziyeh Mohammadi

PII: S0022-2860(17)31248-6

DOI: 10.1016/j.molstruc.2017.09.061

Reference: MOLSTR 24310

To appear in: *Journal of Molecular Structure*

Received Date: 9 March 2017

Revised Date: 11 September 2017

Accepted Date: 18 September 2017

Please cite this article as: M. Amirani Poor, A. Darehkordi, M. Anary-Abbasinejad, M. Mohammadi, Gabapentin-base synthesis and theoretical studies of biologically active compounds: *N*-cyclohexyl-3-oxo-2-(3-oxo-2-azaspiro[4.5] decan-2-yl)-3-arylpropanamides and *N*-(*tert*-butyl)-2-(3-oxo-2-azaspiro[4.5]decan-2-yl)-2-arylacetamide derivatives, *Journal of Molecular Structure* (2017), doi: 10.1016/j.molstruc.2017.09.061.

Graphical Abstract

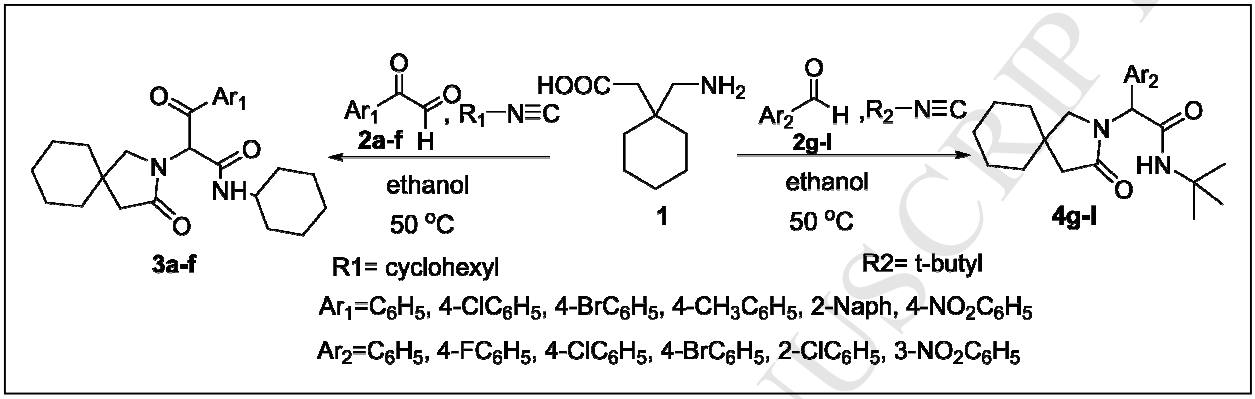

Gabapentin-base synthesis and theoretical studies of biologically active compounds: N-cyclohexyl-3-oxo-2-(3-oxo-2-azaspiro[4.5] decan-2-yl)-3-arylpropanamides and N-(tert-butyl)-2-(3-oxo-2-azaspiro[4.5]decan-2-yl)-2-arylacetamide derivatives

Mahboobe Amirani poor, Ali Darehkordi*, Mohammad Anary-Abbasinejad, Marziyeh Mohammadi

Department of Chemistry, Faculty of Science, Vali-e-Asr University of Rafsanjan, Rafsanjan 77176, Iran

**Corresponding author. Tel.: +98 3431312423; fax: +98 343132429.*

E-mail address: adarehkordi@yahoo.com; darehkordi@mail.vru.ac.

Abstract:

An intermolecular Ugi reaction of 2-(1-(aminomethyl)cyclohexyl)acetic acid (gabapentin) with glyoxal and cyclohexyl isocyanide or aromatic aldehyde and tertbutyl isocyanide under mild conditions in ethanol have been developed to produce two novel class of N-cyclohexyl-3-(aryl)-3-oxo-2-(3-oxo-2-azaspiro[4.5]decan-2-yl)propanamideins and N-(tert-butyl)-2-(3-oxo-2-azaspiro[4.5]decan-2-yl)-2-arylacetamide derivatives in good to excellent yields. This presents the first report for the intermolecular Ugi three component reaction of gabapentin, glyoxal, and an isocyanide. Also according to the theoretical studies the electron-donating groups increase the strength of intramolecular hydrogen bond and electron-withdrawing groups decrease the strength of intramolecular hydrogen bond.

Keyword: Gabapentin, N-Cyclohexyl-3-(aryl)-3-oxo-2-(3-oxo-2-azaspiro[4.5]decan-2-yl)propanamide, Intermolecular Ugi four-center, Theoretical studies, Hydrogen bond

1. Introduction

Multi-component reactions (MCRs) are potent and useful tools for synthesis combinatorial libraries for chemical drug finding [1] and hence new MCRs are being designed for the preparation of new compounds [2]. Multi-component reaction (MCR) contain isocyanide such as Ugi and Passerini reactions are well known and use in medicinal chemistry [3,4]. In the recent years, a new version of the three-component four-center reaction contain isocyanide using an aldehyde and acid has been developed as a bifunctional molecule [5,6].

Ugi multi-component reactions have been used for synthesis of a variety of β-lactam compounds by using β-amino acids, aldehydes, and isocyanides. For example L-aspartic acid α-benzyl ester, enantiopure cyclic β-amino acids, and simple β-amino acids have been extensively used as β-amino acid substrates [7].

In addition to a large number of spiro-compounds have useful biological properties such as anticonvulsant [8], anticancer [9], antibacterial [10], anti-tuberculosis [11], antioxidants [12], also there are in some natural products such as sesquiterpenes and alkaloids and find in living organisms [13] and uses in synthesis of medicinal drugs.

Gabapentin (GBP) is used as an anticonvulsant drug which displays analgesic effects in the therapy of a variety of chronic pain conditions, such as complex regional pain syndrome, inflammatory pain, central pain, trigeminal neuralgia, diabetic neuropathy, headaches, malignant pain, post-herpetic neuralgia, and HIV related neuropathy [14-17]. GBP can also be utilized as an analgesic drug in precautionary analgesia, acute postoperative pain control and shows useful effects on post-operative pain scores enabling the reduction of analgesic consumption after a variety of surgical procedures [18-20]. Also many theoretical studies have been reported on gabapentin molecule which related to structural and medicinal properties [21-23].

According to various medicinal applications as anti-pain and epilepsy and considering above literature reports and in continuing of our studies on the synthesis of bioactive spiro-compounds [24] and also in other to improve the biologically activity of GBP, we have designed and synthesized new N-cyclohexyl-3-(aryl)-3-oxo-2-(3-oxo-2-azaspiro[4,5]decan-2-yl)propanamide derivatives by a simple and efficient synthetic method using a Ugi-three-component reaction involving GBP, various glyoxal and cyclohexyl isocyanide in ethanol (Table 1).

Also in continuing of this research the possibility of intermolecular hydrogen bonding formation between N-H and C=O groups (N-H….O=C) has been surveyed by theoretical calculations for compounds **4a-f**. Because in this series of compounds we can investigate substituent electronical effects on the hydrogen bond strength due to the same position of these substituent on the aromatic ring.

2. Experimental Section

General Methods

All of the chemicals and solvents such as ethyl acetate and ethanol, obtained from Merck Chemical. Co. and were used without further purification. Melting points were determined on a Melt-Tem II melting point apparatus and are uncorrected. Fourier Transform Infrared (FT-IR) spectra were obtained on a Matson-1000 FT-IR spectrometer. Peaks are reported in wavenumbers (cm^{-1}). All Nuclear Magnetic Resonance (NMR) spectra were recorded on a Bruker model DRX-400 AVANCE (^{1}H: 400 MHz) ^{13}C: 100 MHz) NMR spectrometer. Chemical shift are reported in parts per million (ppm) from tetramethylsilane (TMS) as an internal standard in Dimethyl sulfoxide-d6 (DMSO-d_6) as a solvent. Element analyses (C, H, and N) were performed with a Heracus CHN-O-Rapid analyzer. Purity of the compounds was checked by Thin Layer Chromatography (TLC) on Merck silica gel 60 F_{254} percolated sheets in n-Hexane/ethyl acetate mixture and spots were developed using iodine vapors'/ultraviolet light as visualizing agent.

General Procedure for the Synthesis of 3-(aryl)-N-cyclohexyl-3-oxo-2-(3-oxo-2-azaspiro[4.5]decan-2-yl)propanamide (4a-4f)

A mixture of 2-(1-(aminomethyl)cyclohexyl)acetic acid (1 mmol), glyoxal (1 mmol) and cyclohexylisocyanide (1 mmol) in methanol or ethanol (4 ml) was stirred at 50 °C for the appropriate time. The progress of the reaction was monitored by TLC. Upon completion, solvent was removed under reduced pressure and the crude product was purified by washing with n-hexane and diethyl ether to afford the pure 3-(aryl)-N-cyclohexyl-3-oxo-2-(3-oxo-2-azaspiro[4.5]decan-2-yl)propanamide.

General Procedure for the Synthesis of N-(tert-butyl)-2-(aryl)-2-(3-oxo-2-azaspiro[4.5]decan-2-yl)acetamide (4g-4l)

A mixture of 2-(1-(aminomethyl)cyclohexyl)acetic acid (1 mmol), benzaldehyde (1 mmol) and t-butylisocyanide (1 mmol) in methanol or ethanol (4 mL) was stirred at 50 °C for the appropriate time. The progress of the reaction was monitored by TLC. Upon completion, solvent was removed under reduced pressure and the crude product was purified by washing with n-hexane and diethyl ether to afford the pure N-(tert-butyl)-2-(aryl)-2-(3-oxo-2-azaspiro[4.5]decan-2-yl)acetamide.

*N-cyclohexyl-3-oxo-2-(3-oxo-2-azaspiro[4.5]decan-2-yl)-3-phenylpropanamide (***4a***)*

Light yellow, m.p 123-125 ˚C. IR: ν 3253, 2927, 2853, 1684, 1642 cm-1; ^{1}H NMR ($CDCl_3$, 400 MH_Z): δ 7.95 (d, J = 7.6 , 2 H, arom), 7.60 (t, 1 H, J = 8.0 Hz, arom), 7.49 (m, 2 H, arom), 6.38 (s, 1 H, NH), 6.1 (s, 1 H, methine), 3.79 (m, 1 H, methine of cyclohexane), 3.44 (d, J = 10.0 Hz, 1 H_a, CH_2-NH), 3.38 (d, J = 10.0 Hz, 1 H_b, CH_2-NH), 2.31 (d, J = 5.2 Hz, 2 H, CH_2−C=O), 1.93-1.11 (m, 20 H,); ^{13}C NMR ($CDCl_3$, 100 MHz): δ 194.0, 175.1, 164.7, 135.3, 133.8, 130.1, 129.0, 127.3, 60.2, 65.5, 48.7, 43.6, 37.1, 36.9, 36.5, 36.2, 32.8, 32.7, 29.7, 25.5, 25,3, 24,7, 22.7, 22.4 ppm. Elemental analysis: Value calculated for $C_{24}H_{32}N_2O_3$: C, 72.70; H, 8.13; N, 7.06 %, Value found: C, 72.59; H, 8.31; N, 6.96 %,

*3-(4-chlorophenyl)-N-cyclohexyl-3-oxo-2-(3-oxo-2-azaspiro[4.5]decan-2-yl) propanamide (***4b***)*

Light yellow, m.p 181-185 ˚C. IR: ν 3260, 2927, 2853, 1707, 1686 cm^{-1}; ^{1}H NMR ($CDCl_3$, 400 MH_Z): δ 7.86 (d, 2 H, J = 8.0 Hz), 7.38 (d, 2 H, J = 8.0 Hz), 7.00 (s, 1H, NH), 6.23 (S, 1 H, methine), 3.76 (m, 1 H, methine of cyclohexane) 3.53 (d, J = 12.0 Hz, 1 H_a, CH_2-NH), 3.33 (d, J = 12.0 Hz, 1 H_b, CH_2-NH), 2.23 (s, 2 H, CH_2−C=O), 1.87-1.15 (m, 20 H,); ^{13}C NMR ($CDCl_3$, 100 MHz): δ 192.4, 175.1, 164.4, 140.2, 133.4, 129.5, 129.0, 60.6, 56.6, 48.6, 43.7, 37.0, 36.5, 36.4, 32.8, 32.6, 29.7, 25.5, 25.4, 24.6, 22.8, 22.7 ppm. Elemental analysis: Value calculated for $C_{24}H_{31}N_2O_3Cl$: C, 66.89; H, 7.25; N, 6.50 %, Value found: C, 67.01; H, 7.08; N, 6.39 %,

*3-(4-bromophenyl)-N-cyclohexyl-3-oxo-2-(3-oxo-2-azaspiro[4.5]decan-2-yl)propanamide (***4c***)*

Light yellow, m.p 118-120 ˚C. IR: ν 3259, 2927, 2853, 1686, 1644 cm^{-1}; ^{1}H NMR ($CDCl_3$, 400 MH_Z): δ 7.79 (d, 2 H, J = 8.0 Hz), 7.57 (d, 2 H, J = 8.0 Hz), 6.91 (s, 1H, NH), 6.20 (S, 1 H, methine), 3.76 (m, 1 H, methine of cyclohexane) 3.50 (d, J = 12.0 Hz, 1 H_a, CH_2-NH), 3.33 (d, J = 12.0 Hz, 1 H_b, CH_2-NH), 2.30 (s, 2 H, CH_2−C=O), 1.92-1.20 (m, 20 H,); ^{13}C

NMR ($CDCl_3$, 100 MHz): δ 192.7, 175.2, 164.3, 133.9, 132.1, 129.7, 129.0, 60.5, 56.6, 48.7, 43.6, 37.0, 36.7, 36.5, 36.4, 32.8, 32.6, 25.5, 25.4, 24.7, 22.8, 22.7 ppm. Elemental analysis: Value calculated for $C_{24}H_{31}N_2O_3Br$: C, 60.63; H, 6.57; N, 5.89 %, Value found: C, 60.45; H, 6.71; N, 5.77 %,

(4d)

N-cyclohexyl-3-oxo-2-(3-oxo-2-azaspiro[4.5]decan-2-yl)-3-(p-tolyl)propanamide

Light yellow, m.p 150-152 ˚C. IR: ν 32562, 2927, 2853, 1684, 1645 cm^{-1}; ^1H NMR ($CDCl_3$, 400 MH_Z): δ 7.85 (d, 2 H, J = 8.0 Hz), 7.25 (d, 2 H, J = 8.0 Hz), 6.55 (s, 1H, NH), 6.10 (S, 1 H, methine), 3.79 (m, 1 H, methine of cyclohexane) 3.43 (d, J = 12.0 Hz, 1 H_a, CH_2-NH), 3.37(d, J = 12.0 Hz, 1 H_b, CH_2-NH), 2.41 (s, 3 H, CH_3), 2.29 (d, 2 H, J = 4.4 Hz, CH_2−C=O), 1.92-1.15 (m, 20 H,); ^{13}C NMR ($CDCl_3$, 100 MHz): δ 193.4, 175.1, 164.7, 144.9, 132.7, 129.5, 128.4, 60.1, 56.5, 48.7, 43.6, 36.9, 36.7, 36.5, 36.3, 32.8, 32.7, 25.5, 25.4, 24.7, 22.7, 22.7, 21.7 ppm. Elemental analysis: Value calculated for $C_{25}H_{34}N_2O_3$: C, 73.14; H, 8.35; N, 6.82 %, Value found: C, 73.28; H, 8.21; N, 6.93 %.

N-cyclohexyl-3-(naphthalen-2-yl)-3-oxo-2-(3-oxo-2-azaspiro[4.5]decan-2-yl)propanamide

(4e)

Brown powder, m.p 55-58 ˚C. IR: ν 3280, 2927, 2853, 1683, 1645 cm^{-1}; ^1H NMR ($CDCl_3$, 400 MH_Z): δ 8.53(s, 1 H, H_α naph), 7.97-7.52 (m, 6H naph) 6.85 (s, 1H, NH), 6.40 (S, 1 H, methine), 3.70 (m, 1 H, methine of cyclohexane) 3.54 (d, J = 12.0 Hz, 1 H_a, CH_2-NH), 3.41(d, J = 12.0 Hz, 1 H_b, CH_2-NH), 2.23 (s, 2 H, CH_2−C=O), 1.97-1.18 (m, 20 H,); ^{13}C NMR ($CDCl_3$, 100 MHz): δ 193.6, 175.2, 164.7, 135.8, 132.4, 132.4, 130.3, 129.8, 128.8, 128.6, 127.7, 126.9, 123.6, 60.5, 56.7, 48.7, 43.7, 37.0, 36.7, 36.5, 36.3, 32.8, 32.7, 25.5, 25.4, 24.7, 22.8, 22.7 ppm. Elemental analysis: Value calculated for $C_{28}H_{34}N_2O_3$: Elemental Analysis: C, 75.31; H, 7.67; N, 6.27 %, Value found: C, 75.46; H, 7.52; N, 6.39 %,

(4f)

N-cyclohexyl-3-(4-nitrophenyl)-3-oxo-2-(3-oxo-2-azaspiro[4.5]decan-2-yl)propanamide

Yellow, m.p 194 ˚C. IR: ν 3259, 2927, 2853, 1686, 1644 cm^{-1}; ^{1}H NMR ($CDCl_3$, 400 MH_Z): δ 8.45 (d, 2 H, J = 8.0 Hz), 8.34 (d, 2 H, J = 8.0 Hz), 6.91 (s, 1H, NH), 6.20 (S, 1 H, methine), 3.76 (m, 1 H, methine of cyclohexane) 3.50 (d, J = 12.0 Hz, 1 H_a, CH_2-NH), 3.33 (d, J = 12.0 Hz, 1 H_b, CH_2-NH), 2.30 (s, 2H, CH_2−C=O), 1.92-1.20 (m, 20 H,); ^{13}C NMR ($CDCl_3$, 100 MHz): δ 192.0, 175.1, 164.7, 133.3, 132.0, 129.7, 129.0, 60.5, 56.6, 48.7, 43.7, 37.0, 36.7, 36.5, 36.4, 33.0, 32.4, 25.5, 25.4, 24.7, 22.8, 22.7 ppm. Elemental analysis: Value calculated for $C_{24}H_{31}N_3O_5$: C, 65.29; H, 7.08; N, 9.52 %, Value found: C, 65.08; H, 7.23; N, 9.41 %,

(4g)

N-(tert-butyl)-2-(3-oxo-2-azaspiro[4.5]decan-2-yl)-2-phenylacetamide

Light yellow, m.p 144-145 ˚C. IR: ν 3303, 1686, 1667 cm^{-1}; ^{1}H NMR ($CDCl_3$, 400 MH_Z): δ 7.42-7.34 (m, 5 H, arom),), 5.76 (S, 1 H, methine), 5.65 (s, 1H, NH) 3.53 (d, J = 12.0 Hz, 1 H_a, CH_2-NH), 2.77 (d, J = 12.0 Hz, 1 H_b, CH_2-NH), 2.20-2.38 (m, 2 H, CH_2−C=O), 1.56-1.21 (m, 19 H) ; ^{13}C NMR ($CDCl_3$, 100 MHz): δ 174.5, 168.3, 135.1, 129.0, 128.8, 128.3, 58.6, 55.8, 51.7, 43.9, 36.7, 36.5, 36.1, 28.5, 25.6, 22.8, 22.5 ppm. Elemental analysis: Value calculated for $C_{21}H_{30}N_2O_2$: C, 73.65; H, 8.83; N, 8.18 %, Value found: C, 73.51; H, 8.96; N, 8.09 %,

(4h)

N-(tert-butyl)-2-(4-fluorophenyl)-2-(3-oxo-2-azaspiro[4.5]decan-2-yl)acetamide Light brown, m.p 142-144 ˚C. IR: ν 3300, 1668, 1659 cm^{-1}; ^{1}H NMR ($CDCl_3$, 400 MH_Z): δ 7.36-7.33 (m, 2 H), 7.10-7.05 (d, 2 H, J = 8.0 Hz), 5.83 (s, 1H, NH), 5.76 (S, 1 H, methine), 3.50 (d, J = 12.0 Hz, 1 H_a, CH_2-NH), 2.78 (d, J = 12.0 Hz, 1 H_b, CH_2-NH), 2.29 (m, 2 H, CH_2−C=O), 1.55-1.21 (m, 19 H,); ^{13}C NMR ($CDCl_3$, 100 MHz): δ 174.5, 168.16, 163.7, 161.6,

130.5, 115.7, 57.7, 55.7, 51.7, 43.9, 36.7, 36.5, 36.2, 28.6, 25.5, 22.7, 22.6 ppm. Elemental analysis: Value calculated for $C_{21}H_{29}FN_2O_2$: C, 69.97; H, 8.11; N, 7.77 %, Value found: C, 67.09; H, 7.95; N, 7.89 %,

(4i)

N-(tert-butyl)-2-(4-chlorophenyl)-2-(3-oxo-2-azaspiro[4.5]decan-2-yl)acetamide

Light yellow, m.p 164-166 ˚C. IR: ν 3309, 1691, 1662 cm^{-1}; ^1H NMR ($CDCl_3$, 400 MH_Z): δ 7.36-7.29 (m, 4 H), 5.87 (s, 1H, NH), 5.76 (S, 1 H, methine), 3.51 (d, J = 12.0 Hz, 1 H_a, CH_2-NH), 2.78 (d, J = 12.0 Hz, 1 H_b, CH_2-NH), 2.35-2.21 (m, 2 H, CH_2−C=O), 1.54-1.21 (m, 19 H,); ^{13}C NMR ($CDCl_3$, 100 MHz): δ 174.5, 167.9, 134.3, 133.6, 130.2, 129.0, 57.8, 55.8, 51.8, 43.8, 36.7, 36.5, 36.2, 28.6, 25.5, 22.7, 22.6 ppm. Elemental analysis: Value calculated for $C_{21}H_{29}ClN_2O_2$: C, 66.92; H, 7.76; N, 7.43 %, Value found: C, 67.08; H, 7.55; N, 7.59 %,

(4j)

2-(4-bromophenyl)-N-(tert-butyl)-2-(3-oxo-2-azaspiro[4.5]decan-2-yl)acetamide

Light yellow, m.p 164-166 ˚C. IR: ν 3308, 1690, 1663cm^{-1}; ^1H NMR ($CDCl_3$, 400 MH_Z): δ 7.59-7.49 (m, 2 H), 7.29-7.23 (m, 2H), 5.83 (s, 1H, NH), 5.73 (S, 1 H, methine), 3.50 (d, J = 12.0 Hz, 1 H_a, CH_2-NH), 2.78 (d, J = 12.0 Hz, 1 H_b, CH_2-NH), 2.35-2.19 (m, 2 H, CH_2−C=O), 1.56-1.21 (m, 19 H,); ^{13}C NMR ($CDCl_3$, 100 MHz): δ 174.5, 167.9, 134.3, 133.6, 130.2, 129.0, 57.8, 55.8, 51.8, 43.8, 36.7, 36.5, 36.2, 28.6, 25.5, 22.7, 22.6 ppm. Elemental analysis: Value calculated for $C_{21}H_{29}BrN_2O_2$: C, 59.86; H, 6.94; N, 6.65 %, Value found: C, 59.97; H, 6.81; N, 6.78 %,

(4k)

N-(tert-butyl)-2-(2-chlorophenyl)-2-(3-oxo-2-azaspiro[4.5]decan-2-yl)acetamide

Light yellow, m.p 181-184 ˚C. IR: ν 3309, 1671cm^{-1}; ^1H NMR ($CDCl_3$, 400 MH_Z): δ 7.53-7.43 (m, 2 H), 7.35-7.31 (m, 2H), 5.96 (S, 1 H, methine), 5.75 (s, 1H, NH), 3.41(d, J = 12.0

Hz, 1 H_a, CH_2-NH), 2.60 (d, *J* = 12.0 Hz, 1 H_b, CH_2-NH), 2.38-2.19 (m, 2 H, CH_2−C=O), 1.58-1.21 (m, 19 H,); ^{13}C NMR ($CDCl_3$, 100 MHz): *δ* 174.0, 168.3, 134.9, 133.0, 130.1, 130.0, 129.7, 126.9, 56.4, 51.6, 43.6, 36.6, 36.4, 36.3, 28.5, 25.6, 22.7, 22.6 ppm. Elemental analysis: Value calculated for $C_{21}H_{29}ClN_2O_2$: C, 66.92; H, 7.76; N, 7.43 %, Value found: C, 66.81; H, 7.88; N, 7.30 %,

(4l)

N-(tert-butyl)-2-(3-nitrophenyl)-2-(3-oxo-2-azaspiro[4.5]decan-2-yl)acetamide

Light yellow, m.p 231-233 ˚C. IR: ν 3449, 1684, 1630 cm^{-1}; ^{1}H NMR ($CDCl_3$, 400 MH_Z): *δ* 7.53-7.43 (m, 2 H), 7.33-7.31 (m, 2H), 5.95 (S, 1 H, methine), 5.75 (s, 1H, NH), 3.41(d, *J* = 12.0 Hz, 1 H_a, CH_2-NH), 2.59 (d, *J* = 12.0 Hz, 1 H_b, CH_2-NH), 2.38-2.19 (m, 2 H, CH_2−C=O), 1.57-1.23 (m, 19 H,); ^{13}C NMR ($CDCl_3$, 100 MHz): *δ* 174.4, 167.3, 133.9, 133.2, 130.1, 130.0, 128.2, 127.9, 56.1, 51.6, 44.1, 36.6, 36.4, 36.3, 28.5, 25.6, 22.8, 22.5 ppm. Elemental analysis: Value calculated for $C_{21}H_{29}N_3O_4$: C, 65.10; H, 7.54; N, 10.84 %, Value found: C, 65.23; H, 7.40; N, 10.97 %,

Computational methods

The electronic ground state equilibrium geometries of complexes **4a**-**4f** were fully optimized using the M05-2X method with the 6-311++G(d,p) basis set by the Gaussian 09 program package [25]. Frequency calculations were carried out at the same level to ensure that these structures are minima on the potential energy surfaces.

Analysis of the electronic charge density (ρ) and its Laplacian ($\nabla^2\rho$) were done by using the theory of molecular structure suggested by Bader [26]. The calculated electron density, ρ, and its second derivative, $\nabla^2\rho$ were used for describing the nature of the intramolecular N–H···O

hydrogen bond. The atoms in molecules (AIM) [26] analysis was performed using AIM 2000 software [27] at the M05-2X /6-311++G(d,p) level.

The population analysis was carried out by the natural bond orbital (NBO) method [28] at the M05-2X /6-311++G(d,p) level on the optimized structures using NBO program [29] for a better understanding of intramolecular interactions.

3. Results and Discussion

Synthesis

Although recently growing efforts have been made to synthesize and characterize spiro-compounds, but synthesis of these compounds generally less was investigated. In the present work we designed and synthesized a new series of spiro-compounds with potential biological activities by reaction of arylglyoxals or aldehydes and GBP drug with isocyanides.

The glyoxal derivative used in this investigation were prepared in an excellent yield by reaction of aryl methyl ketone derivatives bearing electron-donating, electron-withdrawing, and neutral substituents with selenium dioxide according the literature reported [30] (Scheme 1).

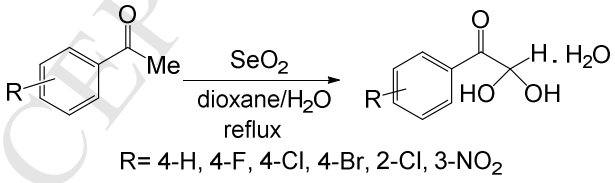

Scheme 1: Synthesis of arylglyoxal derivative

Firstly, we examined the mode coupling of GBP (**1**) with phenylglyoxal (**2**), and isocyanide (**3**) in MeOH as solvent. The reaction carried out smoothly in MeOH at 50 °C to affording the corresponding N-cyclohexyl-3-(aryl)-3-oxo-2-(3-oxo-2-azaspiro[4,5]decan-2-yl)propanamide derivative **4a** in 88% yield after 30 h. The synthetic pathway adopted to obtain the target compounds are presented in Schemes 2.

The effect of the other different solvents such as H_2O, 96% ethanol, absolute ethanol, and ethanol-H_2O, DMF, CH_3CN and THF on the reaction was also examined. We found in

absolute ethanol, the desired product was obtained in 88% yield, while in 96% ethanol, **4a** was isolated in 86% yield (Scheme 2). When the water content in the reaction mixture, was increased, the yield of the product decreased, and using water as the solvent gave very low yields. The reaction GBP (**1**) with phenylglyoxal (**2a**), and cyclohexyl isocyanide (**3**), was also carried out in DMF, THF and CH_3CN solvents under the same conditions. In these solvents desired product was not formed. Although absolute ethanol or methanol produced **4a** in higher yields than with 96% ethanol, but the latter was chosen for this transformation due to the safety, cost, and environmental concerns.

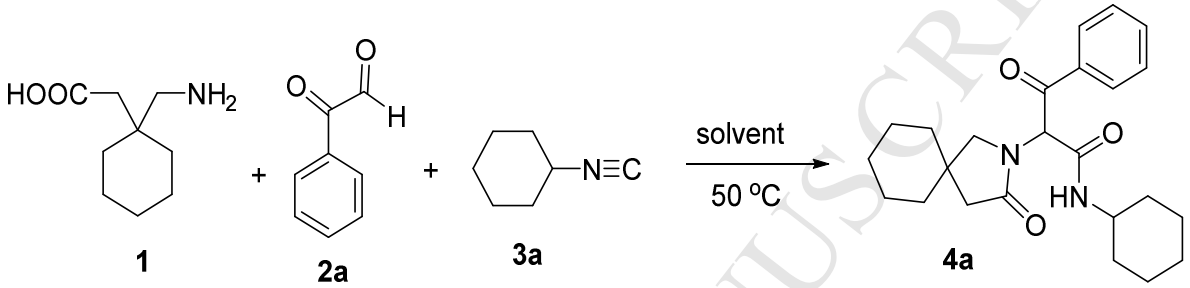

Scheme 2: The mode reaction of GBP (**1**) with phenylglyoxal (**2a**), and isocyanide (**3a**) in various solvents.

To extend the reaction to the other arylglyoxal derivatives and investigation of the substitution effect on the time and yield of reaction, we carried out reaction of GBP and isocyanide with different arylglyoxals. We did not observe any significant change in time and yield of the reaction with changing electron-withdrawing or electron-donating groups substituted on the arylglyoxals.

Interestingly, substituted arylglyoxal with electron-withdrawing groups such as, *p*-fluoro, *p*-bromo, *p*-chloro, *p*-nitro derivatives and substituted arylglyoxal with electron-donating groups such as *p*-methyl each participated effectively in this reaction. In all the cases, the reactions were clean and provided the desired, N-cyclohexyl-3-(aryl)-3-oxo-2-(3-oxo-2-azaspiro[4.5]decan-2-yl)propanamide derivatives in good to excellent yields. The scope and generality of this process are illustrated with different arylglyoxal (Table 1). All products were fully characterized and confirmed by NMR, IR and elemental analysis.

The IR spectrum of N-cyclohexyl-3-oxo-2-(3-oxo-2-azaspiro[4.5]decan-2-yl)-3-phenylpropanamide (**4a**) showed absorption band at 3253 cm^{-1} corresponding to -NH stretching, C-H aromatic and C-H aliphatic stretching appeared at 2927 and 2853 cm^{-1}. Also absorption bands of C=O groups appeared at 1686, 1644 cm^{-1}. The ^{1}H-NMR spectrum of **4a** showed a signal at δ 6.38 ppm corresponding to the NH group, a signal at δ 6.1 ppm, and a multiplet at δ 3.79 ppm

corresponding to the methanes groups. Also the ^{1}H-NMR spectrum of **4a** showed two dublets at δ 3.44 (d, *J* = 10.0 Hz, 1 H), 3.38 (d, *J* = 10.0 Hz, 1 H), corresponding to the –CH_2 (two diastereotopic CH), a multiplet at δ 1.93-1.11 ppm corresponding to cyclohexyl rings CH_2 protons and one dublet at *δ* 7.95 (*J* = 7.6 Hz), a triplet at *δ* 7.60 (*J* = 8 Hz), and one multiplets at δ 7.49 ppm due to the aromatic protons. The ^{13}C-NMR spectrum of **4a** displayed downfield signals at δ 194.0, 175.1 and 164.7 ppm for three carbonyls groups and at δ 135.3, 133.8, 130.1, 129.0, 127.3 ppm for aromatic carbons and 60.2, 65.5, 48.7, 43.6, 37.1, 36.9, 36.6, 36.5, 36.2, 36.1, 32.8, 32.7, 29.7, 25.5, 25.4, 25,3, 24,7, 22.7, 22.4 ppm, for the CH and CH_2 carbons. The IR, ^{1}H-NMR and ^{13}C NMR data for all of the synthesized compounds have been provided in the experimental section.

In continuing of this work we investigated the scope of this reaction with several substituted aldehydes and tert-butyl isocyanide. In this case we select coupling reaction of GBA with benzaldehyde and tert-butyl isocyanide in various solvents as model **(Scheme 3)** . Reaction of GBP and substituted aldehydes with tert-butyl isocyanide in 96% ethanol as a solvent at 50 ^{O}C were successfully produced corresponding product (N-(tert-butyl)-2-(4-aryl)-2-(3-oxo-2-azaspiro[4.5]decan-2-yl)acetamide) in good to excellent yield after 20 h (Table 2).

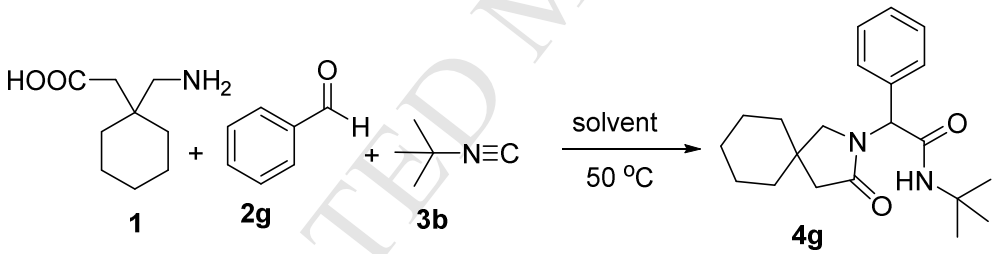

Scheme 3: The mode reaction of GBP (**1**) with benzaldehyde (**2g**), and isocyanide (**3b**) in various solvents

Also all of these products were fully characterized and confirmed by NMR, IR and elemental analysis.

The IR spectrum of N-(tert-butyl)-2-(4-chlorophenyl)-2-(3-oxo-2-azaspiro[4.5]decan-2-yl)acetamide (**4i**) indicated absorption band at 3309 cm^{-1} corresponding to -NH stretching, 2923 and 2848 cm^{-1} , C-H aromatic and C-H aliphatic stretching respectively. Also absorption bands of C=O groups appeared at 1691, 1662 cm^{-1}. The ^{1}H-NMR spectrum of **4i** showed a signal at δ 5.87 ppm corresponding to the NH group, a signal at δ 5.76 ppm corresponding to the methanes groups. Also the ^{1}H-NMR spectrum of **4i** showed two dublets at δ 3.51 (d, *J* = 10.0 Hz, 1 H), 2.78 (d, *J* = 10.0 Hz, 1 H), corresponding to the –CH_2 (two diastereotopic

CH), a multiplet at δ 1.54-1.21 ppm corresponding to tert-butyl protons and cyclohexyl rings CH_2 protons and one multiplets at δ 7.36-7.29 ppm due to the aromatic protons. The ^{13}C-NMR spectrum of **4i** displayed downfield signals at δ 174.5 and 167.9 ppm for carbonyls groups and at δ 134.3, 133.6, 130.2, 129.0 ppm for aromatic carbons and 57.8, 55.8, 51.8, 43.8, 36.7, 36.5, 36.2, 28.6, 25.5, 22.7, 22.6 ppm for the CH_2 and CH_3 carbons. The IR, ^{1}H-NMR and ^{13}C NMR data for all of the synthesized compounds have been provided in the experimental section

A plausible mechanism for reaction of gabapentin with glyoxal and cyclohexyl isocyanide are shown in scheme 4. We assume that the reaction proceeds via the initial formation of imine (**A**) which is formed in situ from reaction of arylglyoxal and GBP. Then the oxo-imine intermediate is attacked by the nucleophilic isocyanide, followed by abstraction of a proton from the carboxylic acid and leading to formation of nitrilium carboxylate (**B**). Subsequent attack of the carboxylate anion on the nitrilium ion generates the cyclic intermediate (**C**), which undergoes a Mumm rearrangement to give the desired lactam **4** (Scheme 4).

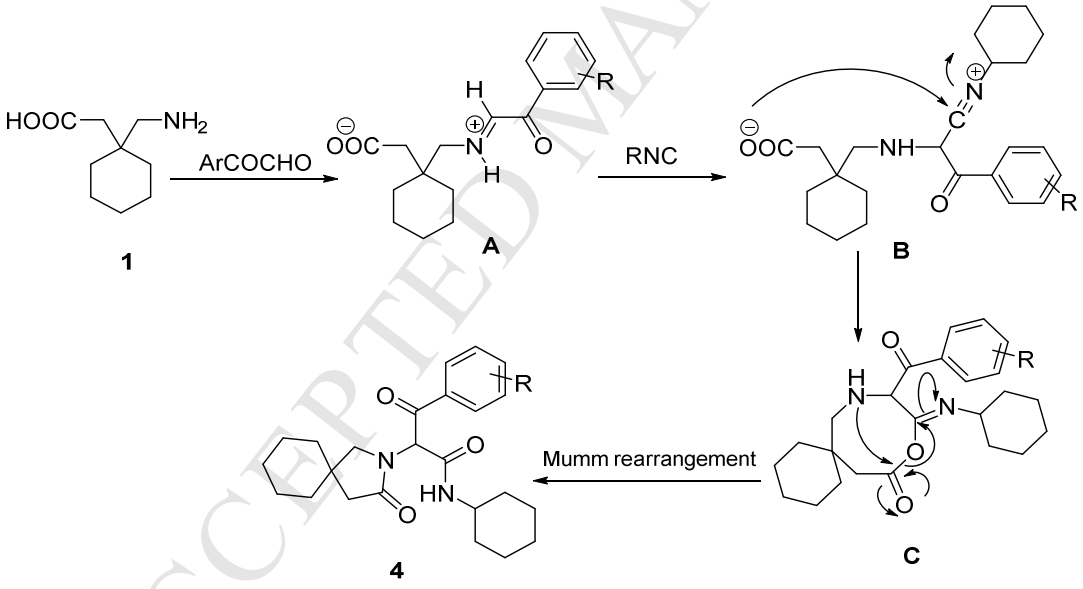

Scheme 4. A plausible reaction pathway.

Table 1: Synthesis of N-cyclohexyl-3-oxo-2-(3-oxo-2-azaspiro[4.5]decan-2-yl)-3-arylpropanamides

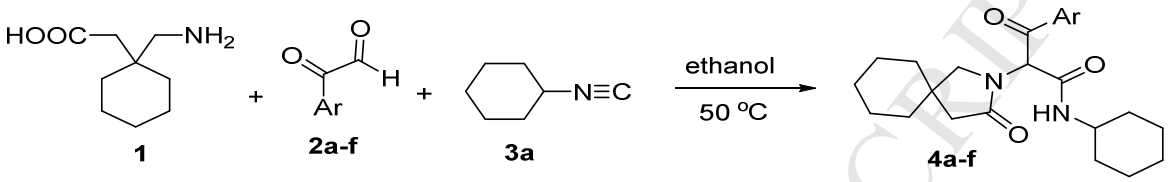

1 + 2a-f + 3a → 4a-f

Entry	Glyoxal	Product	Yield (%)[a]
1	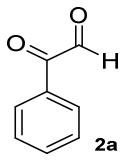 2a	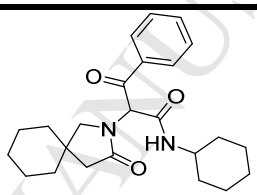 4a	88
2	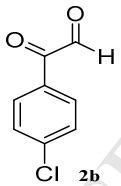 2b	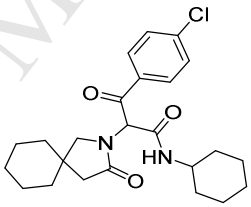 4b	91
3	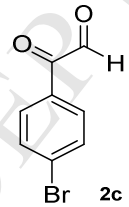 2c	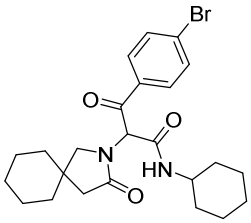 4c	94
4	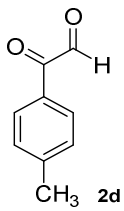 2d	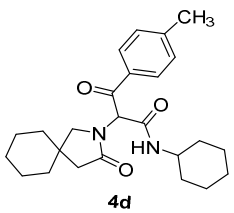 4d	90
5	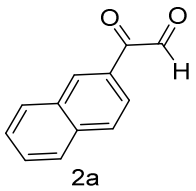 2a	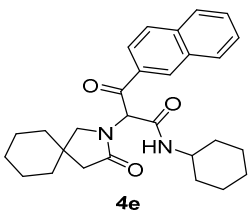 4e	89

6	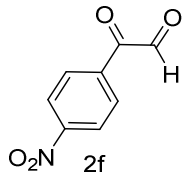 **2f**	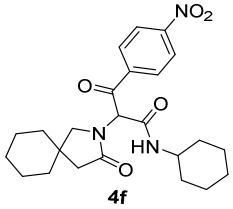 **4f**	**78**

Table 2: Ugi three-component, four-center reaction of a gabapentin with benzaldehydes and t-butylisocyanide

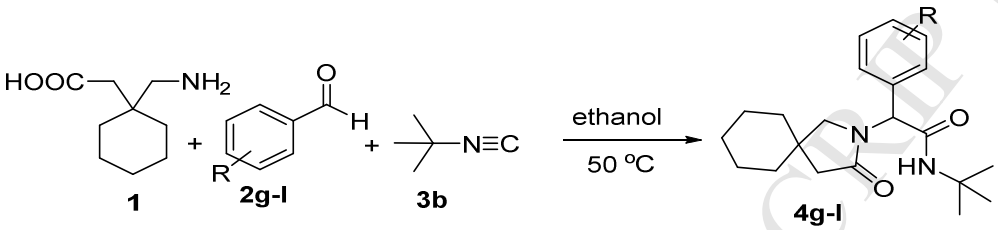

Entry	Aldehyde	Product	Yield (%)[a]
1	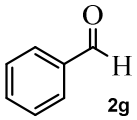 **2g**	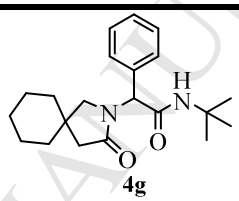 **4g**	**93**
2	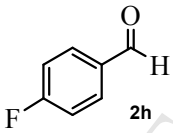 **2h**	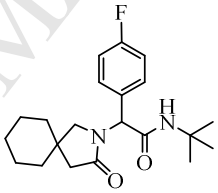 **4h**	**85**
3	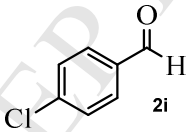 **2i**	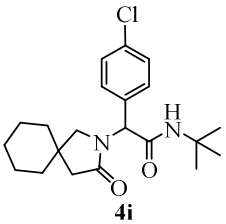 **4i**	**90**
4	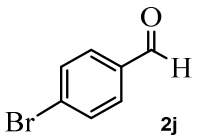 **2j**	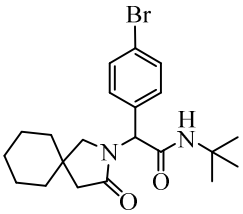 **4j**	**93**
5	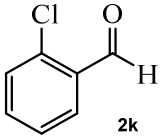 **2k**	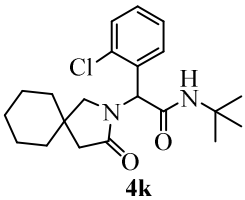 **4k**	**88**

6	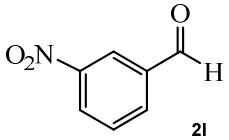 2l	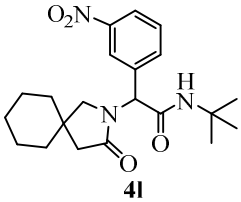 4l	91

[a]Isolated yield

2.2. Theoretical Calculations

Geometrical Parameters:

Most important geometrical parameters, which were optimized at M05-2X /6-311++G(d,p) level of theory are summarized in Table 3.

Table 3. The most important optimized parameters (in Å and degrees) and estimated H-bond energy (kJ mol^{-1})

	$r_{O\cdots H}$	r_{N-H}	$\theta_{N-H\cdots O}$	E_{HB}
4a	2.2417	1.0126	139.194	-12.409
4b	2.2470	1.0127	138.987	-12.252
4c	2.2503	1.0127	138.876	-12.163
4d	2.2451	1.0126	138.997	-12.324
4e	2.2684	1.0126	136.879	-11.853
4f	2.2472	1.0128	139.101	-12.225

As can be seen, The O···H bond length lies in the range of 2.2417–2.2684 Å. Furthermore, the hydrogen bond formation in all complexes is accompanied with elongation of N-H bond and diminishing of O···H intramolecular distance. The minimum and maximum values of O···H bond length correspond to **4a** and **4e**, respectively. The relationship between electron charge density ρ calculated at hydrogen bond critical points (HBCPs) by using AIM and hydrogen bond energy have been reported in the many studies: Stronger H-bond has higher ρ_{HBCP} [26].

The topological analysis of electron densities established by Bader et al. [31-33] can be used to study the nature of hydrogen bond in these complexes. H-bonding can be specified by the change of electron density for the bonded moiety. With formation of an H-bond, the electron density decreases around the proton and proton acceptor, while it increases between the

proton and its acceptor. Bader et al. mentioned that the shared interactions (as covalent and polar bonds) have negative $\nabla^2\rho(r)$ at the BCP commonly corresponds to a local accumulation of electron density into the line of interaction linking the nuclei. In contrast, the closed shell interactions (as ionic bonds or any other interaction between molecules such as van der Waals, medium-weak hydrogen bonding and etc.) have a positive Laplacian and the electron density decreases in the interatomic surface [34].

The total energy density is the sum of potential electronic and the local kinetic energies, V(r) and G(r), respectively, at the BCP [35]

$$H(r_{BCP}) = V(r_{BCP}) + G(r_{BCP})$$

Where the potential energy is correspond to the Laplacian of the electron density by the local form of the virial theorem [36]

$$V(r_{BCP}) = 1/4\nabla^2\rho(r_{BCP}) - 2G(r_{BCP})$$

and the kinetic energy is obtained by partitioning of the electron density [37]

$$G(r_{BCP}) = 3/10(3\pi^2)^{2/3}\rho(r_{BCP})^{5/3} + 1/6\nabla^2\rho(r_{BCP})$$

Cremer and Kraka found that the local kinetic energy density $G(r_{BCP})$ in closed-shell interactions is more than local potential energy density $V(r_{BCP})$. Because the $G(r_{BCP})$ and $V(r_{BCP})$ are everywhere positive and negative respectively, thus $H(r_{BCP}) > 0$. Moreover, the greater of $|V(r_{BCP})|$ caused the greater of the shared character of the interaction and the stability of the structure. It is also viewed that the value of kinetic energy per electron is large ($G(r_{BCP})/\rho(r_{BCP}) > 1$ in atomic units) in closed-shell interactions [38]. A typical molecular graph is shown in Fig. 1.

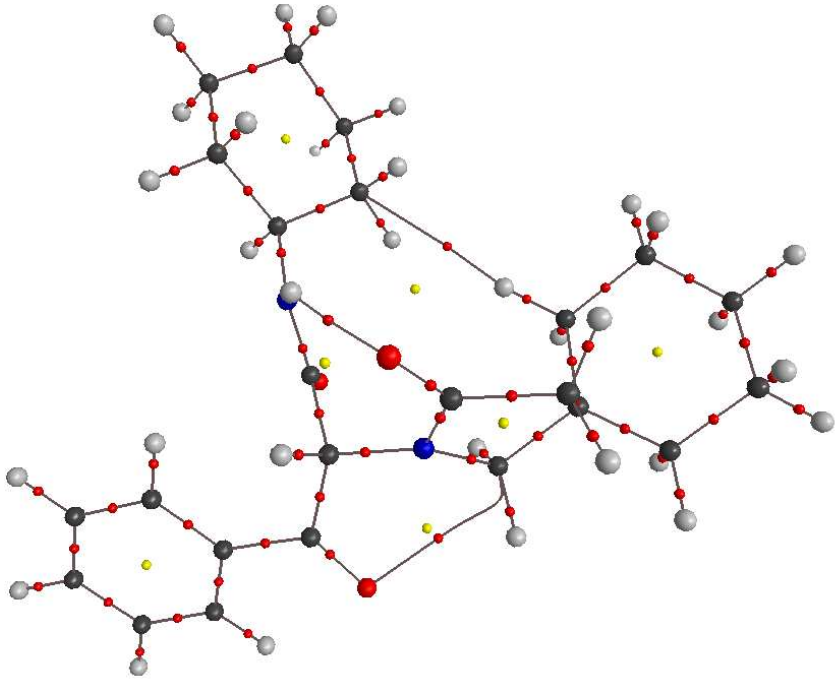

Fig. 1. A typical molecular graph. Small red spheres, small yellow spheres, and lines represent bond critical points (BCP), ring critical points (RCP), and bond paths, respectively.

The values of ρ_{HB}, $\nabla^2\rho_{HB}$, and H_{HB} at the HBCP were determined by the AIM method at the M05-2X/6-311++G(d,p) level of theory (Table 4).

Table 4. Topological electron density properties at O···H bond critical point in atomic unit

	$\rho\times10^2$	$\nabla^2\rho\times10^2$	$H\times10^2$
4a	1.428	4.993	0.1515
4b	1.412	4.933	0.1499
4c	1.403	4.896	0.1488
4d	1.419	4.957	0.1503
4e	1.369	4.741	0.1412
4f	1.410	4.925	0.1500

Rozas et al. [39] suggested that weak H-bonds have $\nabla^2\rho(r_{BCP}) > 0$ and $H_{BCP} > 0$, medium H-bonds are characterized by $\nabla^2\rho(r_{BCP}) > 0$ and $H_{BCP} < 0$ and strong H-bonds reveal $\nabla^2\rho(r_{BCP}) < 0$ and $H_{BCP} < 0$. According to the results, the O···H hydrogen bond in all complexes is classified as weak H- bond. The values of ρ_{HB} lie in the range of 1.369-1.428 e/au^3. The trend in ρ_{HB} is in agreement with geometrical data.

Espinosa et al. in 1998 [40] suggested that the hydrogen-bond energy, E_{HB}, could be extracted from the potential energy density

$E_{HB} = 0.5\ V\ (r_{BCP})$

The values of E_{HB} are reported in Table 1. As can be seen in this table, the values calculated at mentioned level range from -11.853 to -12.409 kj mol^{-1}. Also, the trend in $|E_{HB}|$ is **4a**> **4d**> **4b**> **4f**> **4c**> **4e**. The hydrogen bond interaction energy increased by decreasing $r_{O\cdots H}$ hydrogen bond length. Also, these results are consistent with AIM data.

The E_{HB} values versus $r_{(O\cdots H)}$are shown in Fig. 2.

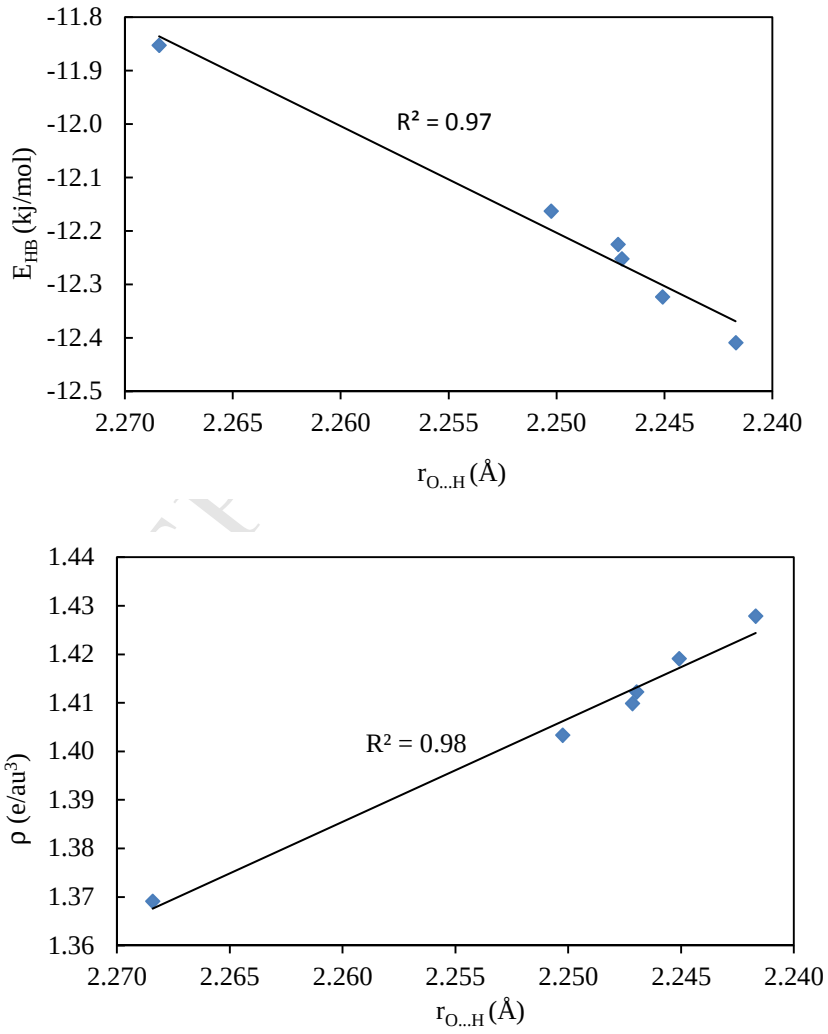

Fig. 2. The linear correlation between **a)** E_{HB} **b)** ρ_{HB} and O···H bond length.

As can be seen, there is a good linear relationship between E_{HB} and r. The correlation coefficient is approximately equal to 0.97. Such a linear relationship is observed between ρ_{HB} and $r_{(O\cdots H)}$(R^2 = 0.98).

The NBO analysis has been performed on the studied complexes at M05-2X /6-311++G(d,p) level. The NBO analysis is a useful tool for describing charge transfer in the interacting orbitals, *i.e.*, changes of charge density in antibonding and lone pair orbitals and also the factors that are responsible for the changes in the internal geometry of the molecule. The NBO calculations show that the most important donor–acceptor interaction is Lp(O) → σ*(N–H). Also, it is observed that the values of both Lp_{1O} → σ*(N–H) and Lp_{2O} → σ*(N–H) interactions were above threshold limit of 0.5 kcal mol^{-1}. The energy values of these interactions ($E^{(2)}$) are gathered in Table 5.

Table 5. Second order perturbation energies $E^{(2)}$ (kcal mol^{-1}) for $LP_O \rightarrow \sigma^*_{NH}$ related to hydrogen bond formation obtained using NBO calculations at M05-2X/6-311++G** level of theory.

	$LP_{(1)\,O} \rightarrow BD^*_{N\text{-}H}$	**$LP_{(2)\,O} \rightarrow BD^*_{N\text{-}H}$**	**Σ**
4a	0.8	1.3	2.1
4b	0.78	1.25	2.03
4c	0.77	1.23	2
4d	0.79	1.28	2.07
4e	0.74	1.19	1.93
4f	0.77	1.24	2.01

The values of total $E^{(2)}$ (Σ) lie in the range of 1.93-2.03 kcal mol^{-1}. The trend in the values of total $E^{(2)}$ is similar to E_{HB}. It is worthwhile to note that there is a correlation between bond length and stabilization energy $E^{(2)}$, *i.e.*, smaller bond lengths (strong hydrogen bonds) have larger stabilization energy.

4. Conclusion

In summary, we have illustrated a new approach for the synthesis of N-cyclohexyl-3-(aryl)-3-oxo-2-(3-oxo-2-azaspiro[4.5]decan-2-yl)propanamides and N-(tert-butyl)-2-(3-oxo-2-azaspiro[4.5]decan-2-yl)-2-arylacetamide derivatives via an Ugi four-center three-component coupling reaction. This method is simple and convenient to produce the N-alkyl-3-(aryl)-3-oxo-2-(3-oxo-2-azaspiro[4.5]decan-2-yl compounds in good to excellent yields from readily available precursors under mild conditions. It is a very useful strategy to produce 2-azaspiro[4.5]decan-4-one derivatives in a single-step process.

Also the results of theoretical studies indicated that the electron-donating groups (CH_3 and Phenyl groups) increase the strength of intramolecular hydrogen bond and electron-withdrawing groups (Cl, Br, NO_2 groups) decrease the strength of intramolecular hydrogen bond. Therefore the electron- donating groups result to conformers' stability and electron-withdrawing groups result to instability of conformers.

Studies on the biologically activities of these compounds are in progress in our laboratory.

Acknowledgements

We gratefully acknowledge, the Vail-e-Asr University of Rafsanjan Faculty Research Grant for financial support.

References

[1]. A. Dömling, Recent developments in isocyanide based multicomponent reactions in applied chemistry, Chem. Rev. 106 (2006) 17-89.

[2]. (a) C. Hulme, V. Gore, Multi-component reactions: emerging chemistry in drug discovery

'From xylocaine to crixivan, Curr. Med. Chem. 10 (2003) 51-80; (b) J.E. Biggs-Houck, A. Younao, J.T. Shaw, Recent advances in multicomponent reactions for diversity-oriented synthesis, Curr. Opin. Chem. Biol. 14 (2010) 371-382.

[3]. I. Ugi, S. Lohberger, R. Karl, The Passerini and Ugi Reactions-4.6. In comprehensive organic synthesis; Trost, B. M., Fleming, I., Eds.; Pergamon Press: Oxford, 2 (1991) 1083-

1106.

[4]. B.B. Toure, D.G. Hall, Natural product synthesis using multicomponent reaction strategies.

Chem. Rev. 109 (2009) 4439-4486.

[5]. A.P. Ilyn, M.V. Loseva, V.Y. Vvedensky, E.B. Putsykina, S.E. Tkachenko, D.V. Kravchenko, V. Khvat, M.Y. Krasavin, A.V. Ivachtchenko, One-Step Assembly of Carbamoyl-Substituted Heteroannelated [1,4]Thiazepines. J. Org. Chem**.** 71 (2006) 2811-
2819.

[6]. M.A. Rasouli, M. Mahdavi, P. Rashidi Ranjbar, M. Saeedi, A. Shafiee, A. Foroumadi, A green one-pot synthesis of N-alkyl-2-(2-oxoazepan-1-yl)-2-arylacetamide derivatives via an Ugi four-center, three-component reaction in water, Tetrahedron Lett. 53 (2012) 7088-7092.

[7]. (a) S. Geday, J.V.d. Eycken, F. Fulop, Liquid-Phase Combinatorial Synthesis of Alicyclic *β*-lactams via Ugi four-component Reaction, *Org. Lett*. 4 (2002) 1967–1969; (b) M. Pirrung, K. D. Sarma, β-Lactam synthesis by Ugi reaction of β-keto acids in aqueous solution, Synlett 8 (2004) 1425–1427; (c) M.C. Pirrung, K.D. Sarma, Multicomponent reactions are accelerated in water, J. Am. Chem. Soc. 126 (2004) 444–445.

[8]. K. Krzysztof, O. Jolanta, D. Malgorzata, physicochemical and anticonvulsant properties of
new *N*-phenylamino derivatives of 2-azaspiro[4.4]nonane- and [4.5]decane-1,3-diones: Part V, Eur. J. Med. Chem. 43 (2008) 53-61.

[9]. C. Young-Won, S. Angela, S. Bao-Ning, M. Qiuwen, C. Hee-Byung, R. Soedarsono, K. Leonardus, R. Agus, F. Norman. S. Steven, K. Douglas, Potential anticancer activity of
naturally occurring and semisynthetic derivatives of aculeatins A and B from Amomum aculeatum, J. Nat. Prod. 3 (2008) 390-395.

[10]. S. van der Sar, J. Blunt, M. Munro, A unique relative of the spirobisnaphthalene class of compounds, Org. Lett. 8 (2006) 2059-2069.

[11]. M.S. Chande, R.S. Verma, P.A. Barve, R.R. Khanwelkar, R.B. Vaidya, K.B. Ajaikumar,
Facile synthesis of active antitubercular, cytotoxic and antibacterial agents: a Michael addition approach, Eur. J. Med. Chem. 40 (2005) 1143-1148.

[12]. B.K. Sarma, D. Manna, M. Minoura, G. Mugesh, Synthesis, structure, spirocyclization mechanism, and glutathione peroxidase-like antioxidant activity of stable spirodiaza selenurane and spirodiazatellurane, J. Am. Chem. Soc. 132 (2010) 5364-5374.

[13]. R. Pradhan, M. Patra, AK. Behera, BK. Mishra, RK. Behera, A synthon approach to spiro

compounds, Tetrahedron 62 (2006) 779-828.

[14]. M. Backonja, A. Beydoun, K.R. Edwards, Gabapentin for the symptomatic treatment of painful neuropathy in patients with diabetes mellitus A randomized controlled trial, JAMA. 280 (1998) 1831-1836.

[15]. T. Gordi, E. Hou, S. Kasichayanula, B. Berner, Pharmacokinetics of gabapentin after a single day and at steady state following the administration of gastric-retentive-extended-

release and immediate-release tablets: A randomized, open-label, multiple-dose, three-way crossover, exploratory study in healthy subjects, Clin. Ther. 2008, 30, 909-916.

[16]. k. Lee, P. Vivithanaporn, R.A. Siamieniuk, H.B. Krentz, F. Maingat, M. Gill, Clinical outcomes and immune benefits of anti-epileptic drug therapy in HIV/AIDS, BMC Neurology 10 (2010) 44-55.

[17]. T. Donovan-Rodriguez, A.H. Dickenson, C.E. Urch, Gabapentin normalizes spinal neuronal responses that correlate with behavior in a rat model of cancer-induced bone pain. Anesthesiology 102 (2005) 132-140.

[18]. U. Srivastava, A. Kumar, S. Saxena, A.R. Mishra, N. Saraswat, S. Mishra, Effect of preoperative gabapentin on postoperative pain and tramadol consumption after minilap open cholecystectomy: a randomized double-blind, placebo-controlled trial, Eur. J. Anesthesiol. 27 (2010) 331-335.

[19]. A. Turan, B. Karamanhoğlu, D. Memiş, P. Usar, Z. Pamukçu, M. Türe, The analgesic effects of gabapentin after total abdominal hysterectomy, Anesth Analg. 98 (2004) 1370-

1373.

[20]. M.L. Rasmussen, O. Mathiesen, G. Dierking, B.V. Christensen, K.L. Hilsted, T.K. Larsen, Multimodal analgesia with gabapentin, ketamine and dexamethasone in combination with paracetamol and ketorolac after hip arthroplasty: a preliminary study, Eur. J. Anesthesiol. 27 (2010) 324-330.

[21]. P.S. Ganeshvar, M. Kanagaraj, S. Gunasekaran, T. Gnanasambandan, Experimental and theoretical investigation of Gabapentin by Density functional theory, IJSER, 7 (2016) 8-15.

[22]. P.G. Vasudev, S. Chatterjee, C. Ramakrishnan, N. Shamala, P. Balaram, Conformational choices for the stereochemically constrained gamma-amino acid

residue gabapentin: theoretical studies and correlation with experimental results, Biopolymers, 92 (2009) 426-435.

[23]. F. Jalali, P.S. Dorraji, H. Mahdiuni, Binding of the neuroleptic drug, gabapentin, to bovine serum albumin: Insights from experimental and computational studies, J. Lumin, 148 (2014) 347-352.

[24]. A. Darehkordi, F. Zand-vakili, A. Talebizadeh R, A novel gabapentin based intermolecular Ugi four-center, three-component reaction for preparing *N*-cyclohexyl-2-

(3-oxo-2-azaspiro[4,5]decan-2-yl)-2-aryl acetamide derivatives, Tetrahedron Lett. 57 (2016) 498-501.

[25]. M.J. Frisch, G.W. Trucks, H.B. Schlegel, G.E. Scuseria, M.A. Robb, J.R. Cheeseman, D.

J. Fox, (2009) Gaussian 09 (Revision A.02). Wallingford, CT: Gaussian.

[26]. R.F.W. Bader, A Suite of programs for the theory of atoms in molecules, hamilton, canada

(contact http://www. chemistry. mcmaster. ca/aimpac) Search PubMed. Atoms in Molecules: A. Quantum Theory, Oxford: Oxford University Press. 75 (1990) 1-49.

[27]. F. Biegler König, J. Schönbohm, Update of the AIM2000-Program for atoms in molecules,

J. Comput. Chem. 23 (2002) 1489-1494.

[28]. A.E. Reed, L. A. Curtiss, F. Weinhold, Intermolecular interactions from a natural bond orbital, donor-acceptor viewpoint, Chem. Rev, 88 (1988) 899-926.

[29]. E.D. Glendening, A.E. Reed, J.E. Carpenter, F. Weinhold, (1998) NBO Version 3.1.

[30]. H.L. Riley, J.F. Morley, N.A.C. Friend, 255. Selenium dioxide, a new oxidising agent. Part I. Its reaction with aldehydes and ketones, J. Chem. Soc. (1932) 1875-1883.

[31]. P.L.A. Popelier, R.F.W. Bader, The existence of an intramolecular C-H-O hydrogen bond

in creatine and carbamoyl sarcosine, Chem. Phys. Lett. 189 (1992) 542-548.

[32]. J.R. Cheeseman, M.T. Caroll, R.F.W. Bader, The mechanics of hydrogen bond formation

in conjugated systems, Chem. Phys. Lett. 143 (1988) 450-458.

[33]. M.T. Caroll, C. Chang, R.F.W. Bader, Prediction of the structures of hydrogen-bonded complexes using the laplacian of the charge density, Mol. Phys. 63 (1988) 387-405.

[34]. R.F.W. Bader, P.J. MacDougall, C.D.H. Lau, Bonded and nonbonded charge concentrations and their relation to molecular geometry and reactivity, J. Am. Chem. Soc. 106 (1984) 1594-1605.

[35]. R.F.W. Bader, P.M. Beddall, Virial field relationship for molecular charge distributions and the spatial partitioning of molecular properties, J. Chem. Phys. 56 (1972) 3320-3329.

[36]. S.B. Boys, F. Bernardi, The calculation of small molecular interactions by the differences of separate total energies. Some procedures with reduced errors, Mol. Phys. 19 (1970) 553-566.

[37]. Yu.A. Abramov, On the possibility of kinetic energy density evaluation from the experimental electron-density distribution, Acta Cryst. A. 53 (1997) 264-272.

[38]. D. Cremer, E. Kraka, Chemical bonds without bonding electron density-does the difference electron-density analysis suffice for a description of the chemical bond, Angew. Chem. 23 (1984) 627-628.

[39]. I. Rozas, I. Alkorta, J. Elguero, Behavior of ylides containing N, O, and C atoms as hydrogen bond acceptors, J. Am. Chem. Soc. 122 (2000) 11154-11161.

[40]. E. Espinosa, E. Molins, C. Lecomte, Hydrogen bond strengths revealed by topological analyses of experimentally observed electron densities, Chem. Phys. Lett. 285 (1998) 170-173.

Research Highlights

- Novel class of azaspiro-compounds were prepared.
- Simple procedure
- High yielding
- Bioactive azaspiro-compounds.